Acta Oncologica, 2011; 50: 806–816

informa
healthcare

ORIGINAL ARTICLE

Radiobiological risk estimates of adverse events and secondary cancer for proton and photon radiation therapy of pediatric medulloblastoma

N. PATRIK BRODIN[1,2], PER MUNCK AF ROSENSCHÖLD[1], MARIANNE C. AZNAR[1], ANNE KIIL-BERTHELSEN[1,3], IVAN R. VOGELIUS[1], PER NILSSON[4], BIRGITTA LANNERING[5] & THOMAS BJÖRK-ERIKSSON[4]

[1]*Radiation Medicine Research Center, Department of Radiation Oncology, Rigshospitalet, University of Copenhagen, Denmark,* [2]*Niels Bohr Institute, Faculty of Sciences, University of Copenhagen, Denmark,* [3]*Department of Clinical Physiology and Nuclear Medicine, Centre of Diagnostic Investigations, Rigshospitalet, University of Copenhagen, Denmark,* [4]*Department of Oncology, Skåne University Hospital and Lund University, Lund, Sweden, and* [5]*Department of Paediatric Oncology, The Queen Silvia Children's Hospital, Gothenburg, Sweden*

Abstract

Introduction. The aim of this model study was to estimate and compare the risk of radiation-induced adverse late effects in pediatric patients with medulloblastoma (MB) treated with either three-dimensional conformal radiotherapy (3D CRT), inversely-optimized arc therapy (RapidArc® (RA)) or spot-scanned intensity-modulated proton therapy (IMPT). The aim was also to find dose-volume toxicity parameters relevant to children undergoing RT to be used in the inverse planning of RA and IMPT, and to use in the risk estimations. *Material and methods*. Treatment plans were created for all three techniques on 10 pediatric patients that have been treated with craniospinal irradiation (CSI) at our institution in 2007–2009. Plans were generated for two prescription CSI doses, 23.4 Gy and 36 Gy. Risk estimates were based on childhood cancer survivor data when available and secondary cancer (SC) risks were estimated as a function of age at exposure and attained age according to the organ-equivalent dose (OED) concept. *Results.* Estimates of SC risk was higher for the RA plans and differentiable from the estimates for 3D CRT at attained ages above 40 years. The risk of developing heart failure, hearing loss, hypothyroidism and xerostomia was highest for the 3D CRT plans. The risks of all adverse effects were estimated as lowest for the IMPT plans, even when including secondary neutron (SN) irradiation with high values of the neutron radiation weighting factors ($WR_{neutron}$). *Conclusions.* When comparing RA and 3D CRT treatment for pediatric MB it is a matter of comparing higher SC risk against higher risks of non-cancer adverse events. Considering time until onset of the different complications is necessary to fully assess patient benefit in such a comparison. The IMPT plans, including SN dose contribution, compared favorably to the photon techniques in terms of all radiobiological risk estimates.

Cancers of the central nervous system (CNS) are, second to lymphomas and leukemias, the most common types of childhood cancers corresponding to 20–30% of all pediatric cases [1,2]. The most common malignant CNS tumor in children is medulloblastoma (MB) which is a primitive neuroectodermal tumor located in the posterior cranial fossa. MBs are characterized by a relatively high rate of spinal metastases at the time of diagnosis [3,4]. The overall five-year survival for standard risk MB (patients with primary tumor in the posterior fossa but without confirmed spinal metastases and with negative cerebrospinal fluid cytology) is 75–85% for children treated with modern day multimodality regimens [5,6]. Treatment consists of surgery followed by post-operative multi-agent chemotherapy and craniospinal irradiation (CSI). Survival rates are relatively high but there are substantial long-term side effects related to radio-chemotherapy of pediatric patients; including loss of hearing or vision,

Correspondence: N. P. Brodin, Department of Radiation Oncology, Section 3994, Rigshospitalet, Blegdamsvej 9, DK-2100 Copenhagen, Denmark. E-mail: brodin.patrik@gmail.com

(Received 15 March 2011; accepted 8 April 2011)

ISSN 0284-186X print/ISSN 1651-226X online
DOI: 10.3109/0284186X.2011.582514

neurocognitive deficits, gonadal dysfunction, cardiopulmonary impairment and endocrine effects [7–16]. The concern regarding therapy-induced secondary cancer (SC) has increased in recent years and is especially relevant for childhood cancer survivors. It has been shown that young age at treatment is associated with an increase in risk for development of most SCs [17,18]. Several approaches have been suggested for estimating the risk of SC induction via different models with dose-responses relating to either linear, linear-exponential or linear-quadratic behavior [19–23]. When comparing results of SC risk estimates from different studies it is vital to consider whether it concerns the risk of contracting a SC or the risk of dying from that SC as this endpoint may vary between studies. It is also important to stratify if the estimates concern lifetime risk or the risk up to a certain attained age as these estimates will differ. Estimating the SC risk on an organ-specific basis would provide the option of assessing whether limiting the dose to the organs most responsible for SC induction can lower the total SC risk.

The prescribed CSI dose has been successfully decreased from 36 Gy to 23.4 Gy in standard-risk MB patients without compromising survival rates [24]. Provided that the disease is properly staged as either standard or high risk, the treatment regimen can be stratified accordingly. Common to both standard- and high-risk patients is that the CSI treatment is followed by a boost to the primary tumor site (posterior cranial fossa) up to 54–55 Gy [5]. Since radiotherapy can be given with varying prescribed CSI doses it is warranted to consider the impact of this variation in estimations of treatment-related long-term complications. There is lack of general consensus on the lateral extent of the spinal part of the target volume. Including the entire vertebral column is a viable option as this prevents asymmetric spinal growth. This is based on the findings that bone growth is inhibited at absorbed doses above approximately 20 Gy [25].

Today the standard technique for CSI is three-dimensional conformal radiotherapy (3D CRT). This technique results in irradiation of a large volume of normal tissue to high doses. Several studies have investigated the feasibility of CSI with intensity-modulated radiotherapy (IMRT) or proton therapy and the estimated effect on SC risk [21,26–28].

This study was aimed at estimating and comparing SC risk and risks of several other non-cancer long-term complications between 3D CRT, rotational IMRT and spot-scanned intensity-modulated proton therapy (IMPT). The aim was also to use the inverse optimization tools in IMRT and IMPT to purposely limit the dose to most organs at risk (OARs), as an attempt at radiobiological treatment optimization for pediatric MB. Using the full potential of the different treatment techniques in this way allows for a realistic comparison of modalities. The treatment plans and risk estimations were performed for varying CSI prescription doses and spinal target volumes in order to gain some perspective into the effect of these variations on long-term complications.

Material and methods

Patient material and treatment planning

Ten pediatric patients, four males and six females, ages 4 to 15 years (mean age 8 years), were included in this study. They had all received CSI for MB at the Copenhagen University Hospital in 2007–2009. The craniospinal clinical target volume (CTV) was defined as comprised of a cranial CTV consisting of the whole brain and a spinal CTV defined as the spinal canal extending caudally to the S2-S3 junction. Target volume definitions were based on computed tomography (CT) scans. The craniospinal planning target volume (PTV) consisted of the cranial CTV with a 5 mm isotropic margin and the spinal CTV with a 7 mm isotropic margin. An alternative PTV was created with the spinal part consisting of the entire vertebral column with 3 mm lateral margins. This alternative PTV was not considered for the main analysis but rather to test how different definitions of spinal target volume would affect the risk estimates. To facilitate treatment planning comparison, prescription doses were set as 23.4 Gy and 36 Gy to the craniospinal PTV. The fractionation scheme was chosen as 1.8 Gy/fraction for all prescription levels and each prescription regimen was followed by boost treatment to a total dose of 54 Gy to the boost PTV comprised of the posterior cranial fossa with a 5 mm isotropic margin.

All treatment plans were generated using the Eclipse treatment planning system version 8.9 (Varian Medical Systems, Palo Alto, CA). The different techniques were normalized to all have the same mean target dose as the 3D CRT plans, in order to facilitate objective plan comparison. The 3D CRT plans were created with two lateral opposed cranial fields. The caudal edge of these fields was positioned just above the cranial edge of the patient's shoulders in order to protect the thyroid gland. The eyes were shielded by MLC-leaves but only to the extent that it did not compromise PTV coverage. Additionally, a spinal posterio-anterior field encompassing the spinal part of the PTV was applied. The junction between the cranial and spinal fields was

moved 1.0 cm caudally once in the 23.4 Gy prescription regimen and twice in the 36 Gy regimen to limit over or under dosage due to possible set-up variations in a clinical treatment setting. In order to assess the importance of the lateral extent of the spinal target volume in 3D CRT, multiple plans were created with varying spinal field widths. For the different plans the multi-leaf-collimator (MLC) leaves were fitted to the spinal PTV with 0.5 cm, 0.75 cm, 1.0 cm and 1.5 cm lateral margins, respectively. When reviewing the treatment records of the patients, the 1.0 cm leaf-to-PTV margin corresponded best to the set-up in which most of the patients had been treated. This margin was chosen when comparing the 3D CRT plans to the other techniques. The boost plans were created using four fields, two opposing fields from the right and left sides along with two wedged fields incident from a more posterior direction.

Rotational IMRT plans were created using the RapidArc® (RA) technique (Varian Medical Systems, Palo Alto, CA). RA plans consisted of a cranial arc covering the whole brain and the cranial part of the spinal canal down to the C2 or C3 vertebra. The rest of the spinal canal was covered by a spinal arc delivering radiation from a posterior 140 degree arc only to avoid unnecessary irradiation through the arms and ventral parts of the patient. There was substantial overlap between the cranial and spinal arcs to facilitate an intensity-modulated junction that was less sensitive to set-up error than a sharp junction between field edges. Two spinal arcs were used in the case where the cranio-caudal extent of the spinal canal exceeded the span of a single arc. The boost plans consisted of a 220 degree arc covering the boost PTV without irradiating through the anterior parts of the head.

IMPT plans were generated with machine data corresponding to a PT2 Varian proton therapy system utilizing active spot-scanning. The plans were generated using three fields incident from the posterior direction. A range shifter can be introduced when necessary, in order to reach both shallow and deeply situated structures in the body. The range shifter effectively lowers the span of the achievable nominal energy, which is 70–250 MeV for this machine, and thus decreasing the depth to which the protons reach. The IMPT plans consisted of one field with a range shifter covering most of the spinal canal and two fields, of which one had a range shifter, covering the brain and the cranial part of the spinal canal. The junction between the IMPT fields was set with an overlap and modulated between fields as for the RA technique. The boost plans consisted of a single posterior field with a range shifter to ensure full coverage of the posterior fossa. Figure 1 illustrates the difference in dose distribution relating to the different treatment techniques.

Proton radiotherapy exposes the patient to secondary neutron (SN) irradiation which is not considered in the treatment planning system hence this extra dose contribution was added manually. This was done by using organ-specific neutron doses corresponding to a spot-scanned proton beam taken from the study by Newhauser et al. [26]. In that study the neutron dose contribution was simulated using Monte Carlo methods for a pediatric mathematical phantom receiving craniospinal proton irradiation. A limitation of using this data is that SNs are assumed to be generated within the patient only. This will underestimate the SN contribution, especially when a range shifter is applied as the beam passing through the range shifter will induce SNs. In order to account for possible uncertainty in the relative biological effectiveness (RBE) of SNs, neutron radiation weighting factors

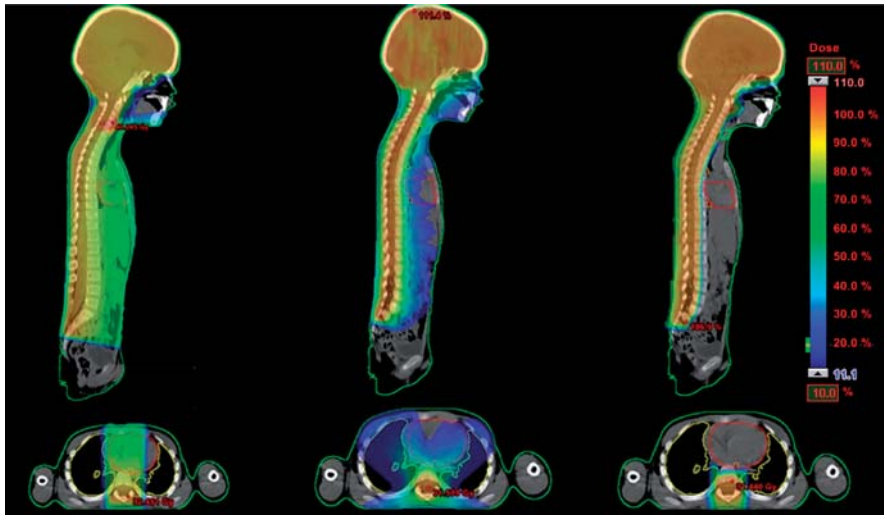

Figure 1. Dose distributions in the sagittal and transversal plane related to treatment with (from left) 3D CRT, RapidArc and IMPT.

($WR_{neutron}$) five times higher than the energy-dependent values recommended in ICRP publication 92 were used as a sensitivity analysis [29].

The inverse planning optimization for RA and IMPT was focused on lowering the risk of treatment-induced complications by limiting the dose to as many critical structures as possible. The actual optimization objectives were set with the aim of fulfilling the dose objectives proposed in Table I, when possible. The data shown in Table I are the results of an extensive literature search focused on finding dose tolerance levels relevant for pediatric MB patients. The dose objectives and the inter-organ priority were based on the references given in Table I and the preferences of experienced physicians in pediatric- and general oncology (BL, TBE). The main difference between RA and IMPT optimization was the fact that most of the OARs did not receive any absorbed dose from the protons as the distal edge of a beam is very sharp.

Modeling of secondary cancer risk and non-cancer adverse effects

A concept for phenomenological modeling of SC risks is that of organ equivalent dose (OED) which was developed by Schneider et al. in 2005 [22]. This provides a single measure of an OED in Gy which represents the often heterogeneous dose distribution of a dose-volume histogram (DVH). This value represents the uniform dose that would yield the same SC risk to an organ as the inhomogeneous dose distribution described in the DVH. An alternative way of estimating OED was presented by Schneider et al. in 2008 based on the combined SC data of Hodgkin's disease patients having undergone radiotherapy and that of the atomic bomb survivors extrapolated to higher doses more relevant to radiotherapy [30]. The authors fitted this data to OED models with a linear, linear-exponential (bell-shaped) and plateau dose-response, although the linear model did not provide a good fit to data. There is evidence from large clinical studies of SC that does not support a decrease in risk at high radiotherapy doses [31,32]; the plateau-model thus appears to be a more appropriate selection/model. Even with appropriate models the uncertainties in SC risk estimates are considerable. When faced with clinical decisions one needs to consider the differences, for example between modern treatment and that given several decades ago and the possible variations in genetic cancer susceptibility between the atomic bomb survivors and modern day cancer patients.

The OED for the plateau-model was calculated as

$$\mathrm{OED}_{\mathrm{org}} = \frac{1}{N}\sum_{i=1}^{N}\frac{1-e^{-\delta_{\mathrm{org}}D_i}}{\delta_{\mathrm{org}}} \tag{1}$$

where δ_{org} is the organ-specific dose-response parameter derived from fitting the model to the Hodgkin's cohort data. D_i is the dose to bin i in the DVH and N is the total number of dose bins. To test the sensitivity of the SC risk on the choice of model, estimates were also made with the bell shaped and linear models from Schneider et al. [30] as a comparison. The excess absolute risk (EAR) of SC was estimated as a linear function of the OED adjusted for population-specific variables according to Equation 2.

$$\mathrm{EAR}(D,e,a,s) = \beta\,\mathrm{OED}\mu(e,a,s) \tag{2}$$

The parameter μ represents the population-specific risk modification and is a function of age at exposure, e, attained age, a and gender, s, and β describes the initial slope of the dose-response curve [30].

$$\mu(e,a,s) = \exp\left[\gamma_e(e-37)+\gamma_a\ln\left(\frac{a}{46}\right)\right]\cdot(1\pm s)$$
$$+\ \textit{for females}, -\ \textit{for males} \tag{3}$$

The constants γ_e and γ_a are related to attained age and age at exposure and were derived from fitting the model to the original data. The cumulative EAR of developing a SC was then estimated to a given attained age by taking into account competing risks of death according to Equation 4.

$$C_{\mathrm{EAR}}(a) = \sum_{i=e+1}^{a}\mathrm{EAR}(D,e,i,s)\cdot\frac{S(i)}{S(e)} \tag{4}$$

The ratio $S(i)/S(e)$ represent the gender-specific conditional probability of a person alive at age e to reach age i. The survival functions were taken from Kellerer et al. [33].

A limitation of the model by Schneider et al. is that no organ-specific model parameters were derived in the original publication [30]. The dose-response curve relates to the induction of any solid secondary cancer, thus representing the mean dose-response for all secondary cancers studied. In order to calculate the organ-specific risk contribution, the dose-response was assumed to be valid for all studied organs.

To take the risk contribution from each of the relevant organs into account, a weighted mean OED was calculated for all organs for which incidence of radiation-induced cancers was published in the Life Span Study (LSS) [34]. The weighted mean OED was calculated based on the data provided in Table II according to Equation 5.

$$\mathrm{OED}_{\text{weighted mean}} = \frac{\mathrm{OED}_{\text{Esophagus}} \cdot \mathrm{Incidence}_{\text{Esophagus}} + \mathrm{OED}_{\text{Stomach}} \cdot \mathrm{Incidence}_{\text{Stomach}} + \ldots}{\mathrm{Incidence}_{\text{Esophagus}} + \mathrm{Incidence}_{\text{Stomach}} + \ldots} \quad (5)$$

Table I. Organ-specific dose objectives relating to children treated with radiation therapy.

Irradiated organ	Endpoint	Patient data	Chemo	NTCP-model	Priority	Dose objectives	Reference
Bone Marrow	Hematologic toxicity	Children	Yes	N/A	2	$D_{mean,non\text{-}target\ bone} < 10$ Gy	**Chang et al. (2002)**
Eyes	Cataract	Children	N/A	N/A	2	$D_{max,eye} < 20$ Gy or BED (mean eye dose) < 40 $Gy_{0.65}$	**Kal et al. (2009)**
	Dry eyes	Children	Yes	N/A	2	$D_{max,eye} < 20$ Gy or BED (mean eye dose) < 40 $Gy_{0.65}$	**Whelan et al. (2010)**
	Double vision	Children	Yes	N/A	2	$D_{max,eye} < 20$ Gy or BED (mean eye dose) < 40 $Gy_{0.65}$	**Whelan et al. (2010)**
	Blindness	Children	Yes	N/A	2	$D_{max,eye} < 20$ Gy or BED (mean eye dose) < 40 $Gy_{0.65}$	**Whelan et al. (2010)**
	Cataract	Children	Yes	N/A	2	$D_{mean,temp.\ lobe} < 30$ Gy	**Whelan et al. (2010)**
	Dry eyes	Children	Yes	N/A	2	$D_{mean,temp.\ lobe} < 30$ Gy	**Whelan et al. (2010)**
	Double vision	Children	Yes	N/A	2	$D_{mean,temp.\ lobe} < 30$ Gy	**Whelan et al. (2010)**
	Blindness	Children	Yes	N/A	2	$D_{mean,temp.\ lobe} < 30$ Gy	**Whelan et al. (2010)**
	Cataract	Children	Yes	N/A	2	$D_{mean,temp.\ lobe} < 30$ Gy	**Whelan et al. (2010)**
Heart	Cardiac failure	Children	Yes	N/A	1	$D_{mean,heart} < 3.5$ Gy	**Guldner et al. (2006)**
	Ejection Fraction	Children	Yes	N/A	1	$D_{mean,heart} < 3.5$ Gy	**Guldner et al. (2006)**
	End Systolic Wall Stress	Children	Yes	N/A	1	$D_{mean,heart} < 3.5$ Gy	**Guldner et al. (2006)**
	Long-term cardiac mortality	Adults	Yes	Relative seriality	1	$D_{mean,heart} < 3.5$ Gy	**Gagliardi et al. (1996)**
Liver	Radiation Induced Liver Disease	Adults	No	LKB	1	$D_{mean,liver} < 10$ Gy	**Dawson et al. (2005)**
	Radiation Induced Liver Disease	Adults	No	LKB	1	$D_{mean,liver} < 10$ Gy	**Xu et al. (2006)**
	Radiation Induced Liver Disease	Adults	No	LKB	1	$D_{mean,liver} < 10$ Gy	**Xu et al. (2006)**
Neurocognitive effects	IQ decrease	Children	Yes	IQ-decline	2	$D_{mean,whole\ brain} < 25$ Gy $D_{mean,sup.tent.\ brain} < 25$ Gy	**Merchant et al. (2008)**
	Diffrent neurologic sequelae	Children	N/A	N/A	-	-	**Goldsby et al. (2010)**
Parotids	Xerostomia (75% flow rate red.)	Adults	N/A	LKB	3	$EUD_{parotid} < 14$ Gy	**Houweling et al. (2009)**
	Xerostomia (75% flow rate red.)	Adults	N/A	LKB	3	$EUD_{parotid} < 14$ Gy	**Roesink et al. (2001)**
	Xerostomia (50% flow rate red.)	Adults	N/A	N/A	3	$EUD_{parotid} < 14$ Gy	**Bussels et al. (2004)**
Endocrine system	Hypothyroidism	Children	Yes	N/A	5	$D_{mean,thyroid} < 6$ Gy	**Ricardi et al. (2001)**
	Hypothyroidism	Adults	Y & N	N/A	5	$D_{mean,thyroid} < 6$ Gy	**Bathia et al. (1996)**
	Hypothyroidism	Children	Yes	N/A	4	$D_{mean,pituitary} < 20$ Gy	**Chow et al. (2009)**
	Neurologic sequelae	Children	Yes	N/A	-	-	**Xu et al. (2004)**
	Sitting height	Children	Yes	N/A	-	-	**Xu et al. (2004)**
	ACTH deficiancy	Children	Yes	N/A	-	-	**Rose et al. (2005)**
Gynecological	Infertility	Children	Yes	N/A	3	$D_{mean,testis} < 7.5$ Gy & $D_{mean,hypothal/pituitary} < 40$ Gy	**Green et al. (2010)**
	Infertility	Children	Yes	N/A	3	$D_{mean,ovaries} < 5.0$ Gy & $D_{mean,hypothal/pituitary} < 30$ Gy	**Green et al. (2009)**
	Radiation induced menopause	Children	Yes	N/A	3	$D_{mean,ovaries} < 5.0$ Gy & $D_{mean,hypothal/pituitary} < 30$ Gy	**Chiarelli et al. (1999)**
	Infertility	Children	Yes	N/A	3	$D_{max,uterus} < 10$ Gy	**SFRO (2008)**†
Kidneys	Chronic renal dysfunction	Children	N/A	N/A	1	BED_{Kidney} (mean dose) < 16 $Gy_{2.5}$	**Kal et al. (2009)**
	Renal toxicity	Children	N/A	N/A	1	BED_{Kidney} (mean dose) < 16 $Gy_{2.5}$	**Esiashvili et al. (2009)**
Lungs	Restrictive lung function	Children	No	N/A	1	$D_{mean,lung} < 10$ Gy	**Attard-Montalto et al. (1992)**
	Pulmonary diffusion capacity	Children	Yes	N/A	1	$D_{mean,lung} < 10$ Gy	**Bossi et al. (1997)**
	Pulmonary function reduced	Children	No	N/A	1	$D_{mean,lung} < 10$ Gy	**Weiner et al. (2006)**
	Pneumonitis	Adults	Yes	Mean Lung Dose	1	$D_{mean,lung} < 10$ Gy	**Marks et al. (2010)**
Hearing apparatus	Ototoxicity	Children	Yes	N/A	2	$D_{mean,cochlea} < 37$ Gy	**Miettinen et al. (1997)**
	Ototoxicity	Children	Yes	N/A	2	$D_{mean,cochlea} < 37$ Gy	**Huang et al. (2002)**
Submandibular glands	Xerostomia (75% flow rate red.)	Adults	N/A	N/A	5	$D_{mean,submandib.\ glands} < 19$ Gy	**Murdoch-Kinch et al. (2008)**
Chiasm	Blindness	Children	Yes	N/A	2	$D_{max,chiasm} < 52$ Gy & $V_{50} < 100\%$	**SFRO (2008)**†
Optic nerve	Blindness	Children	Yes	N/A	2	$D_{max,optic\ nerve} < 50$ Gy	**SFRO (2008)**†
Skin	Telangiectasia/Epilation	Children	Yes	N/A	5	$D_{max,skin} < 35$ Gy	**SFRO (2008)**†
Brainstem	Necrosis	Children	Yes	N/A	1	$D_{max,brainstem} < 54$ Gy	**SFRO (2008)**†
Esophagus	Esophagal RTOG Grade 1-4 tox	Adults	Y & N	N/A	3	$D_{max,esophagus} < 40$ Gy	**Ahn et al. (2005)**
Larynx	Laryngeal edema	Adults	Y & N	LKB-EUD	3	$EUD_{larynx} < 29$ Gy	**Rancati et al. (2009)**

†Referenced publication is based on the gathered clinical experience of the Société Française de Radiothérapie Oncologique (SFRO), not on published clinical data, published as *Guide des procedures de radiotherapie externe 2007* in 2008.
EUD, Equivalent Uniform Dose, further explanation given with corresponding reference.
Inter-organ priorities were based on:
1 - Permanent, life threatening event with no possible medical substitution of organ function.
2 - Permanent, non-life threatening event with inability to lead an independent life, medical substitution not possible.
3 - Permanent effect with possibility of partial medical substitution.
4 - Permanent effect with possibility of full medical substitution but with likely complications.
5 - Permanent effect with possibility of complication free full substitution.

Table II. Radiation-related secondary cancer incidence from the LSS [34] and as adopted in this study. The incidence is given as average excess absolute risk due to external low-LET radiation as per 10 000 person years and Sieverts equivalent dose.

	Incidence $(10^4\ PYSv)^{-1}$		Values adopted $(10^4\ PYSv)^{-1}$	
Site/cancer type	Males	Females	Males	Females
Esophagus	0.26	0.44	0.26	0.44
Stomach	2.61	5.86	2.61	5.86
Colon	2.66	1.01	2.66	1.01
Liver	0.033	0.005	0.033	0.005
Lungs	2.67	5.81	2.67	5.81
Bone and connective tissue	0.38	0.12	–	–
Skin	0.89	0.72	0.89	0.72
Female breast	–	6.80	–	6.80
Prostate	0.44	–	0.44	–
Urinary bladder	0.84	1.02	0.84	1.02
Brain and CNS	–0.21	0.43	0.00	0.43
Thyroid	0.87	2.32	0.87	2.32
Non-Hodgkin 's lymphoma	0.73	–0.20	–	–
Hodgkin's disease	0.04	0.04	–	–
Multiple myeloma	0.26	–0.08	–	–
Leukemia	3.35	2.29	–	–

As the ability of organ-specific SC risk estimation is dependent of knowing where a SC might occur, the cancer types where no localized anatomical site relating to radiation exposure could be specified were excluded (shown in italics). An attempt was made at estimating the risk of secondary leukemia but no model could be found that well predicts the risk as a function of radiation dose [35]. We thus estimate the risk of contracting a localized solid SC. Negative values in Table II are interpreted as zero and thus not contributing to the secondary cancer risk.

Modeling of non-cancer normal tissue complication probabilities (NTCP) was done according to the radiation dose-response functions presented in Table III. The basic rationale of NTCP modeling is to use the dose-response relationship of a complication derived from a patient cohort and apply it as a predictor of complication rate in other patients. This is used to define dose limits for OARs that should keep the risk of complications at an acceptable level. Although NTCP modeling can be a powerful tool in treatment planning, the model parameters are associated with considerable uncertainty. Relative comparison of pairs of treatment plans or modalities are however less sensitive to these uncertainties than absolute risk estimates.

Results

The estimations in Figure 2 show that the SC risk is highest for the RA treatments but the difference between the photon techniques does not become apparent until attained ages above 40 years, representing a latency period since treatment of about 30 years. The estimate of solid SC risk at an attained age corresponding to the average lifetime of a Danish person (78.5 years) was 45%, 56% and 7% for 3D CRT, RA and IMPT, respectively, for 23.4 Gy prescribed CSI dose. The corresponding risks for the 36 Gy CSI dose were 54%, 71% and 9%. These results were compared with the corresponding EARs estimated with a bell shape and a linear model as shown in Figure 3. It is shown that the choice of model does affect the absolute risk estimates especially for the RA plans. The absolute estimates depend strongly on the initial slope of the different dose-response curves. The EAR estimate at an attained age of 78.5 years was lower for RA than for 3D CRT

Table III. Dose-response functions and corresponding model parameters utilized in the estimation of treatment-induced non-cancer adverse effects.

Studied endpoint	Model	Model parameters	References
Hypothyroidism	Logistic function*	$b_0 = -2.50$ $b_1 = 0.09$	Bathia et al. [40]
Ototoxicity (Hearing loss)	Logistic function*	$b_0 = -7.34$ $b_1 = 0.148$	Huang et al. [8]
Pneumonitis	Logistic function*	$b_0 = -3.87$ $b_1 = 0.126$	Marks et al. [41]
Heart failure	Linear-quadratic function $OR = 1 + \alpha_1 \cdot D_{mean} + \alpha_2 \cdot D^2_{mean}$	$\alpha_1 = 0.19$ $\alpha_2 = 0.002$	Guldner et al. [38]
Xerostomia	LKB-model†	$TD_{50} = 39.9$ Gy $m = 0.40$ $n = 1$	Houweling et al. [42]
Blindness	Linear function $P = 0.0028 \cdot BED_{2.5,\,mean} - 0.0015$	–	Whelan et al. [7]
Chronic renal failure	Linear function $P = 0.075 \cdot BED_{2.5,\,mean} - 1.42$	–	Kal et al. [43]

*$P = e^{b_0+b_1 \cdot D_{mean}} / 1 + e^{b_0+b_1 \cdot D_{mean}}$

†Lyman-Kutcher-Burman model, details described elsewhere [44].

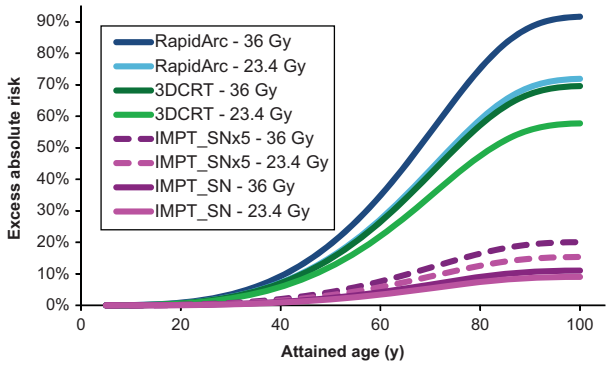

Figure 2. Mean values for all 10 patients of cumulative solid secondary cancer risk as a function of attained age for the three different treatment modalities studied. Results are given for the two different prescription CSI dose levels that are relevant for this patient group. The results are shown up to an attained age of 100 years, after this the cumulative risk levels out since the probability of surviving to older ages is very low. For IMPT the results are given as including SN dose with values of the $WR_{neutron}$ as proposed in ICRP publication 92, denoted IMPT_SN and values five times higher, denoted IMPT_SNx5.

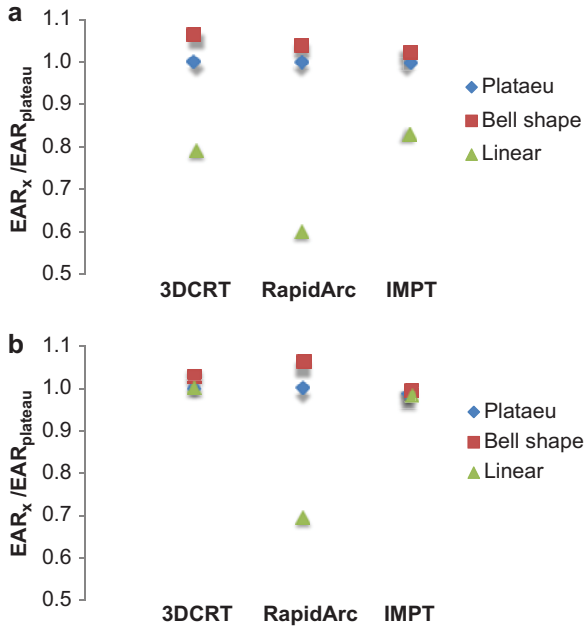

Figure 3. Mean values of EAR are given for a plateau, bell shape and a linear model, normalized to the EAR of the plateau model. The estimates are given for prescribed CSI doses of a) 23.4 Gy and b) 36 Gy. The relative difference between models depends on the initial slope of the dose-response curves and at what doses the risk plateaus out/turns over. The linear model deviates somewhat from the other two, likely since it did not provide a good fit to the original input data.

according to the linear model, 33% vs. 36% for the 23.4 Gy CSI dose and 50% vs. 54% for the 36 Gy CSI dose. This is attributable to the fact that the mean doses to the SC critical structures were lower with RA and any linear model will thus favor RA over 3D CRT for these patients because of the direct relationship to mean dose.

It is shown that the excess absolute SC risk estimated for IMPT is affected by a large variation in the neutron RBE. The risk is however substantially lower with IMPT than for both photon techniques even with high values of $WR_{neutron}$.

Figure 4 shows the results of the NTCP estimations calculated according to Table III. The risk of inducing heart failure, xerostomia, hypothyroidism and ototoxicity was estimated as substantially higher for 3D CRT than for RA. The risk of pneumonitis was equivalent for the two photon techniques while the risk of inducing blindness was slightly higher for the RA plans. All NTCP estimates were lower with IMPT compared to the photon techniques even though the results in Figure 4 are presented for the IMPT_SNx5 plans. The risk of developing ototoxicity was shown to be higher for the lower CSI prescription dose for the RA plans. This was due to the boost plans with RA yielding a higher dose to the cochlea per prescription Gy than the main craniospinal plans. The estimates of chronic renal failure were not shown since the kidney doses were sufficiently low to not yield any considerable risk of renal failure; the highest estimate for any plan was below 2%. As NTCP estimates are subject to uncertainty, the absolute values should be considered somewhat cautiously with more emphasis on the relative comparison between modalities.

The risk of inducing heart failure was considerably higher for 3D CRT compared to the other two techniques. The effect on this endpoint of varying the spinal field widths was studied separately and shown in Figure 5. The risk of heart failure increases with spinal field width since the mean heart dose becomes larger. This shows that depending on the choice of field set-up in 3D CRT the risk of inducing heart failure is 2–2.5 times higher than that of RA.

Table IV represents target coverage parameters for the three different treatment techniques normalized to the same mean craniospinal PTV dose. The cranial target coverage was slightly better with 3D CRT compared to RA. The lack of conformity in the 3D CRT plans was shown by the high value of $V_{107\%}$ in the spinal CTV and the low scores in conformity index.

Discussion

The results of this study show the estimated radiobiological differences between 3D CRT, RA and IMPT in the treatment of pediatric MB. As expected the solid SC risk was higher for intensity-modulated photon treatment compared to 3D CRT. The EAR estimates are relatively high but we believe that this is the case for pediatric MB patients. Estimates are in reasonable accordance with the study by Mu et al.,

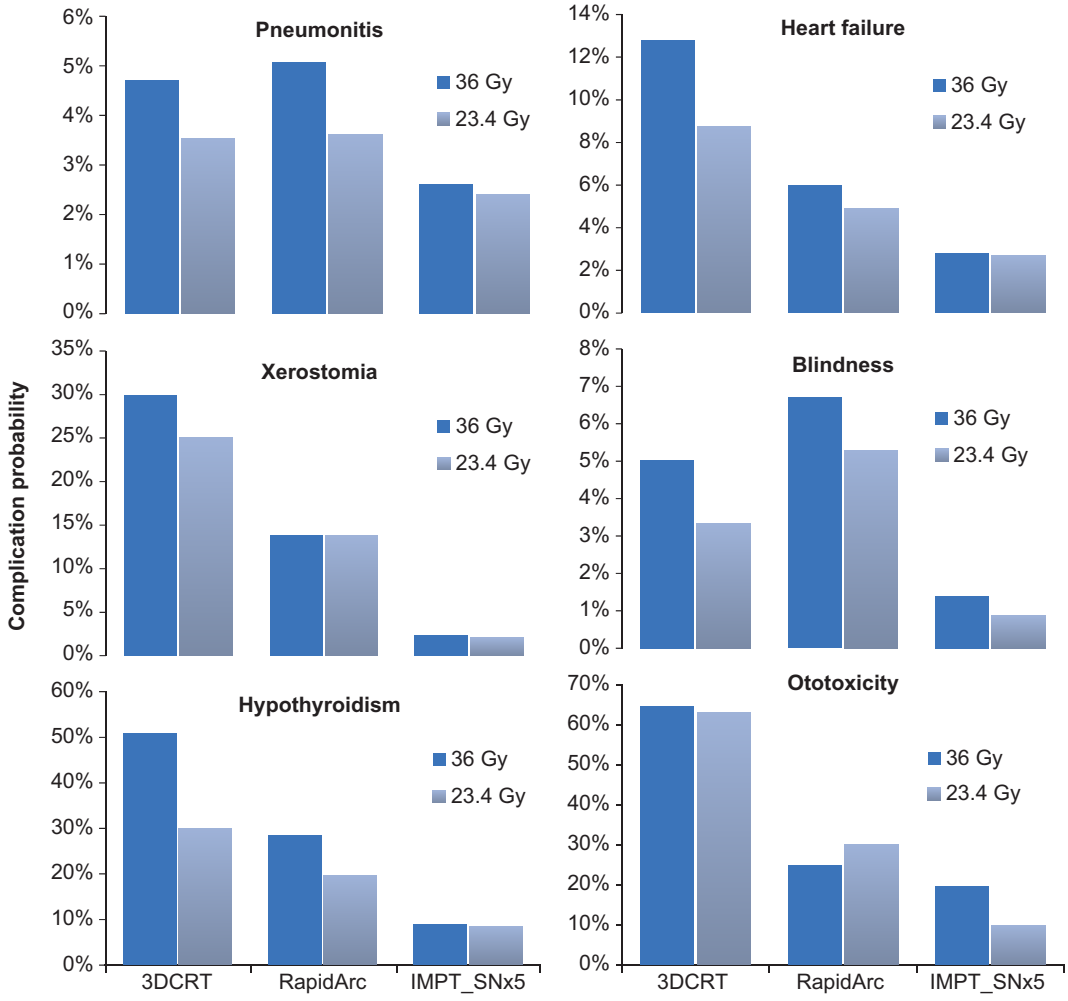

Figure 4. Mean values for all 10 patients comparing long-term risks of inducing pneumonitis, heart failure, xerostomia, blindness, hypothyroidism and ototoxicity between the different treatment modalities.

who also focused on pediatric MB. They estimated the lifetime risk of contracting a lethal SC to be 20% for 3D CRT and 30% for IMRT relating to a 23.4 Gy CSI prescription dose [21]. In the study by Miralbell et al. the yearly risk of SC induction was estimated for a 3-year-old MB patient to 0.76%, 0.43% and 0.05% for 3D CRT, IMRT and proton therapy, respectively [36]. This would correspond to respective lifetime risks of 55%, 31% and 4%, their estimates were based on a prescribed dose to the craniospinal axis of 36 Gy. The high risk related to 3D CRT in their study was likely attributed to the very young age of the patient as the treatment field would cover a large proportion of such a small body. A recent study estimated the long-term mortality in childhood cancer survivors based on the current follow-up of the childhood cancer survivor study (CCSS) cohort [37]. The authors showed that compared to other pediatric cases, MB patients were at high risk of SC mortality despite the fact that MB patients were the most prone to die from late recurrences.

Estimates of SC risk are in general subject to considerable uncertainty and often affected by the choice of model as shown in Figure 3, so the absolute estimates should be treated with caution. However, relative comparisons between treatment modalities can likely be more reliably considered. Treating children with IMRT, whether rotational or fixed-field,

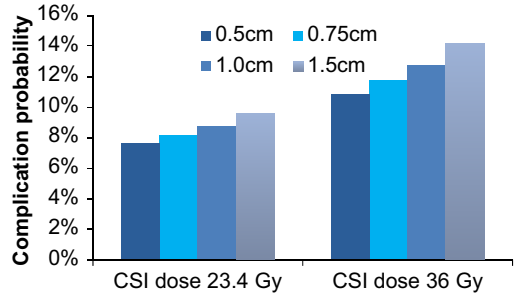

Figure 5. Mean values of all 10 patients comparing the risk of heart failure for different spinal field widths in 3D CRT treatment.

Table IV. Mean values for all ten patients of target coverage parameters comparing the 3D CRT, RapidArc and IMPT plans for the 23.4 Gy craniospinal prescription dose.

Parameter	PTV craniospinal	PTV boost	CTV - Brain	CTV - Spinal
3D CRT				
D_{min}	13.5 Gy	45.1 Gy	21.5 Gy	21.3 Gy
D_{max}	29.5 Gy	57.3 Gy	25.0 Gy	28.6 Gy
V_{95}	96.6%	99.3%	99.9%	98.7%
V_{107}	4.5%	0.0%	0.1%	17.1%
CI	0.61	0.61	–	–
RapidArc				
D_{min}	15.5 Gy	41.1 Gy	19.6 Gy	21.0 Gy
D_{max}	27.8 Gy	59.4 Gy	27.7 Gy	25.9 Gy
V_{95}	95.2%	97.8%	97.3%	98.7%
V_{107}	6.3%	3.9%	7.5%	0.7%
CI	0.73	0.77	–	–
IMPT				
D_{min}	13.7 Gy	39.2 Gy	19.4 Gy	22.1 Gy
D_{max}	26.5 Gy	59.0 Gy	26.3 Gy	24.8 Gy
V_{95}	97.1%	98.6%	99.7%	99.5%
V_{107}	0.2%	0.2%	0.2%	0.0%
CI	0.89	0.90	–	–

CI: Conformity Index. Closer to unity equals better conformity, calculation details described elsewhere [45].

should because of the underlying uncertainties still be considered as somewhat controversial.

The time since exposure aspect needs to be considered when trying to estimate actual patient detriment and when the late effects are most likely to occur. As modern, highly conformal, radiotherapy techniques are more commonly used, the definition of target volume becomes increasingly important. If, for example the entire vertebral column is included as PTV to receive at least 20 Gy we found that the SC risk was slightly increased for the RA plans and nearly doubled for the IMPT plans (data not shown). This results in weighting the risk of asymmetrical spinal growth, i.e. scoliosis, against that of an increased risk of SC. For such a comparison it is vital to consider at what ages the different complications are most likely to occur.

As for the risk estimations for non-cancer adverse effects, the results suggest that patients treated with 3D CRT are subject to substantially higher risks of serious complications such as heart failure and severe hearing loss compared to those treated with intensity-modulated therapy. The choice between the two photon techniques thus appears to be a choice between higher SC risk or higher risk of non-cancer adverse events. The basis for these risk comparisons lies in mathematical modeling and the inherit uncertainties need to be considered if the estimates are to guide clinical decision making. There is also the consideration of which technique provides the most robust treatment. A problem in 3D CRT treatment of MB is that it uses junctions between fields, risking over/under dosage due to uncertainties in treatment set-up. Intensity-modulated treatment would not suffer from the same problem since the field junctions can be modulated with intentional overlap between different fields. An error in treatment set-up would in this situation lead to only a small dose variation compared to the sharp junctions in 3D CRT.

The estimates of heart failure are based on patients that were treated with radiation therapy and anthracyclin chemotherapy, which also contributes to the risk of heart failure [38]. The radiotherapy related heart failure risk was about five times higher (data not shown) for 3D CRT compared to RA attributable to a large difference in mean heart dose (18.9 Gy vs. 7.3 Gy for the 36 Gy CSI dose). It is difficult to assess which risks are of greatest importance for the future of these patients. It might, for example be worse to have a 10% risk of developing heart failure before the age of 40 years than a 30% risk of contracting a SC before turning 60. Early results of comparing the effect of different long-term complications on a common scale have recently been shown and appear promising [39]. Estimating risks at old ages for people having survived a cancer in childhood is particularly difficult. This is primarily due to that cohorts in large studies like the CCSS [18] have not yet reached the ages where the general population incidence of cancer and heart complications becomes large. Increasing follow-up in, for example the CCSS will hopefully reveal whether the relative risks at older ages continue to be elevated, or whether they will decrease as the general population incidence increases.

In this work the optimization priority of normal tissue toxicity prevention was based solely on the severity of the different endpoints. The best treatment plans with respect to these risks would likely also include consideration of the incidence of the different complications. This would prevent the optimizer from trying to reduce a risk which is already negligible. We also attempted to optimize the RA plans with respect to SC risk by lowering the dose to the organs suggested as responsible for SC induction presented in Table II. This resulted in lower estimates of solid SC risk but unfortunately also in some deterioration of spinal target coverage. Such an optimization approach should thus preferably be accompanied by assessment of tumor control probability.

The risks of all long-term complications, cancer and non-cancer alike, were shown to be considerably lower for IMPT than for the photon techniques. Pediatric MB thus seems to be an obvious candidate to recommend for proton therapy if available. The risk estimation for the IMPT plans is made difficult by uncertainty in the RBE of SN produced by the proton beam. The conclusions for IMPT as favorable

over photon therapy were however shown in this study to hold even for high values of neutron RBE. This suggests that SN irradiation does not warrant the choice of photon therapy over proton therapy for MB. At least if proton therapy is given with IMPT with neutron contamination intensity as that used in the presented work, although the estimates are likely somewhat underestimated for the fields with range shifters. Passively scattered proton beams tend to yield more SN and needs to be investigated separately.

This study provided estimates and comparisons of solid secondary cancer risk and risks of non-cancer late complications for three different radiotherapy techniques for treatment of pediatric MB. The uncertainties involved in the estimates should be considered, especially when interpreting the absolute risk estimates. The results of this study have shown that treating pediatric MB patients with 3D CRT would subject them to higher risks of several severe late complications compared to RA treatment. This shows the potential of intensity-modulated therapy in limiting the dose to important risk organs for these patients. The risk of SC induction was however estimated as higher if treated with RA compared to 3D CRT. This study also provided SC risk estimates as a function of attained age, highlighting the importance of considering at what ages different risks are most likely to occur.

Acknowledgements

This work was supported by funding from the Danish Childhood Cancer Foundation. The authors would like to thank chief physicians Catherine Rechnitzer and Karsten Nysom at the Department of Paediatric Oncology at Rigshospitalet, Copenhagen, for their support of this project. The authors would also like to thank everyone in the research group at the Radiation Oncology Department at Rigshospitalet, Copenhagen, for their valued input and discussions.

Declaration of interest: Per Munck af Rosenschöld has a research agreement with Varian Medical Systems. The authors alone are responsible for the content and writing of the paper.

References

[1] Parkin DM, Kramarova E, Draper GJ, Masuyer E, Michaelis J, Neglia J, et al. International incidence of childhood cancer. Lyon: International Agency for Research on Cancer; 1998.

[2] Steliarova-Foucher E, Stiller C, Kaatsch P, Berrino F, Coebergh JW, Lacour B, et al. Geographical patterns and time trends of cancer incidence and survival among children and adolescents in Europe since the 1970s (the ACCIS-project): An epidemiological study. Lancet 2004;364(9451): 2097–105.

[3] Kortmann RD, Kuhl J, Timmermann B, Mittler U, Urban C, Budach V, et al. Postoperative neoadjuvant chemotherapy before radiotherapy as compared to immediate radiotherapy followed by maintenance chemotherapy in the treatment of medulloblastoma in childhood: Results of the German prospective randomized trial HIT '91. Int J Radiat Oncol Biol Phys 2000;46:269–79.

[4] Zeltzer PM, Boyett JM, Finlay JL, Albright AL, Rorke LB, Milstein JM, et al. Metastasis stage, adjuvant treatment, and residual tumor are prognostic factors for medulloblastoma in children: Conclusions from the Children's Cancer Group 921 randomized phase III study. J Clin Oncol 1999; 17:832–45.

[5] Skowronska-Gardas A. A literature review of the recent radiotherapy clinical trials in pediatric brain tumors. Rev Recent Clin Trials 2009;4:42–55.

[6] Taylor RE, Bailey CC, Robinson K, Weston CL, Ellison D, Ironside J, et al. Results of a randomized study of preradiation chemotherapy versus radiotherapy alone for non-metastatic medulloblastoma: The International Society of Paediatric Oncology/United Kingdom Children's Cancer Study Group PNET-3 Study. J Clin Oncol 2003;21: 1581–91.

[7] Whelan KF, Stratton K, Kawashima T, Waterbor JW, Castleberry RP, Stovall M, et al. Ocular late effects in childhood and adolescent cancer survivors: A report from the childhood cancer survivor study. Pediatr Blood Cancer 2010;54:103–9.

[8] Huang E, Teh BS, Strother DR, Davis QG, Chiu JK, Lu HH, et al. Intensity-modulated radiation therapy for pediatric medulloblastoma: Early report on the reduction of ototoxicity. Int J Radiat Oncol Biol Phys 2002;52:599–605.

[9] Merchant TE, Kiehna EN, Li C, Shukla H, Sengupta S, Xiong X, et al. Modeling radiation dosimetry to predict cognitive outcomes in pediatric patients with CNS embryonal tumors including medulloblastoma. Int J Radiat Oncol Biol Phys 2006;65:210–21.

[10] Mertens AC, Yasui Y, Liu Y, Stovall M, Hutchinson R, Ginsberg J, et al. Pulmonary complications in survivors of childhood and adolescent cancer. A report from the Childhood Cancer Survivor Study. Cancer 2002;95:2431–41.

[11] Weiner DJ, Maity A, Carlson CA, Ginsberg JP. Pulmonary function abnormalities in children treated with whole lung irradiation. Pediatr Blood Cancer 2006;46:222–7.

[12] Hancock SL, McDougall IR, Constine LS. Thyroid abnormalities after therapeutic external radiation. Int J Radiat Oncol Biol Phys 1995;31:1165–70.

[13] Heikens J, Michiels EM, Behrendt H, Endert E, Bakker PJ, Fliers E. Long-term neuro-endocrine sequelae after treatment for childhood medulloblastoma. Eur J Cancer 1998; 34:1592–7.

[14] Green DM, Kawashima T, Stovall M, Leisenring W, Sklar CA, Mertens AC, et al. Fertility of female survivors of childhood cancer: A report from the childhood cancer survivor study. J Clin Oncol 2009;27:2677–85.

[15] Green DM, Kawashima T, Stovall M, Leisenring W, Sklar CA, Mertens AC, et al. Fertility of male survivors of childhood cancer: A report from the Childhood Cancer Survivor Study. J Clin Oncol 2010;28:332–9.

[16] Mulrooney DA, Yeazel MW, Kawashima T, Mertens AC, Mitby P, Stovall M, et al. Cardiac outcomes in a cohort of adult survivors of childhood and adolescent cancer: Retrospective analysis of the Childhood Cancer Survivor Study cohort. BMJ 2009;339:b4606.

[17] Ng AK, Kenney LB, Gilbert ES, Travis LB. Secondary malignancies across the age spectrum. Semin Radiat Oncol 2010;20:67–78.
[18] Meadows AT, Friedman DL, Neglia JP, Mertens AC, Donaldson SS, Stovall M, et al. Second neoplasms in survivors of childhood cancer: Findings from the Childhood Cancer Survivor Study cohort. J Clin Oncol 2009;27: 2356–62.
[19] Dasu A, Toma-Dasu I, Olofsson J, Karlsson M. The use of risk estimation models for the induction of secondary cancers following radiotherapy. Acta Oncol 2005;44:339–47.
[20] Kry SF, Salehpour M, Followill DS, Stovall M, Kuban DA, White RA, et al. The calculated risk of fatal secondary malignancies from intensity-modulated radiation therapy. Int J Radiat Oncol Biol Phys 2005;62:1195–203.
[21] Mu X, Bjork-Eriksson T, Nill S, Oelfke U, Johansson KA, Gagliardi G, et al. Does electron and proton therapy reduce the risk of radiation induced cancer after spinal irradiation for childhood medulloblastoma? A comparative treatment planning study. Acta Oncol 2005;44:554–62.
[22] Schneider U, Zwahlen D, Ross D, Kaser-Hotz B. Estimation of radiation-induced cancer from three-dimensional dose distributions: Concept of organ equivalent dose. Int J Radiat Oncol Biol Phys 2005;61:1510–5.
[23] Schneider U, Kaser-Hotz B. Radiation risk estimates after radiotherapy: Application of the organ equivalent dose concept to plateau dose-response relationships. Radiat Environ Biophys 2005;44:235–9.
[24] Gajjar A, Chintagumpala M, Ashley D, Kellie S, Kun LE, Merchant TE, et al. Risk-adapted craniospinal radiotherapy followed by high-dose chemotherapy and stem-cell rescue in children with newly diagnosed medulloblastoma (St Jude Medulloblastoma-96): Long-term results from a prospective, multicentre trial. Lancet Oncol 2006;7:813–20.
[25] Eifel PJ, Donaldson SS, Thomas PR. Response of growing bone to irradiation: A proposed late effects scoring system. Int J Radiat Oncol Biol Phys 1995;31:1301–7.
[26] Newhauser WD, Fontenot JD, Mahajan A, Kornguth D, Stovall M, Zheng Y, et al. The risk of developing a second cancer after receiving craniospinal proton irradiation. Phys Med Biol 2009;54:2277–91.
[27] Taddei PJ, Mirkovic D, Fontenot JD, Giebeler A, Zheng Y, Kornguth D, et al. Stray radiation dose and second cancer risk for a pediatric patient receiving craniospinal irradiation with proton beams. Phys Med Biol 2009;54:2259–75.
[28] Yoon M, Shin DH, Kim J, Kim JW, Kim DW, Park SY, et al. Craniospinal irradiation techniques: A dosimetric comparison of proton beams with standard and advanced photon radiotherapy. Int J Radiat Oncol Biol Phys Epub 2010 Oct 5.
[29] ICRP. Relative biological effectiveness (RBE), quality factor (Q), and radiation weighting factor (w(R)). Ann. ICRP: (Oxford: International Commission on Radiological Protection); 2003. Report No.: 92.
[30] Schneider U, Walsh L. Cancer risk estimates from the combined Japanese A-bomb and Hodgkin cohorts for doses relevant to radiotherapy. Radiat Environ Biophys 2008;47: 253–63.
[31] Travis LB, Hill DA, Dores GM, Gospodarowicz M, van Leeuwen FE, Holowaty E, et al. Breast cancer following radiotherapy and chemotherapy among young women with Hodgkin disease. JAMA 2003;290:465–75.
[32] Chaturvedi AK, Engels EA, Gilbert ES, Chen BE, Storm H, Lynch CF, et al. Second cancers among 104,760 survivors of cervical cancer: Evaluation of long-term risk. J Natl Cancer Inst 2007;99:1634–43.
[33] Kellerer AM, Nekolla EA, Walsh L. On the conversion of solid cancer excess relative risk into lifetime attributable risk. Radiat Environ Biophys 2001;40:249–57.
[34] UNSCEAR. Report to the General Assembly: Sources and effects of ionizing radiation. Annex I - Epidemiological evaluation of radiation-induced cancer. 2000.
[35] Allard A, Haddy N, Le Deley MC, Rubino C, Lassalle M, Samsaldin A, et al. Role of radiation dose in the risk of secondary leukemia after a solid tumor in childhood treated between 1980 and 1999. Int J Radiat Oncol Biol Phys Epub 2010 Mar 18.
[36] Miralbell R, Lomax A, Cella L, Schneider U. Potential reduction of the incidence of radiation-induced second cancers by using proton beams in the treatment of pediatric tumors. Int J Radiat Oncol Biol Phys 2002;54:824–9.
[37] Yeh JM, Nekhlyudov L, Goldie SJ, Mertens AC, Diller L. A model-based estimate of cumulative excess mortality in survivors of childhood cancer. Ann Intern Med 2010;152: 409–17.
[38] Guldner L, Haddy N, Pein F, Diallo I, Shamsaldin A, Dahan M, et al. Radiation dose and long term risk of cardiac pathology following radiotherapy and anthracyclin for a childhood cancer. Radiother Oncol 2006;81:47–56.
[39] Brodin NP, Vogelius IR, Maraldo MV, Aznar MC, Kiil-Berthelsen A, Björk-Eriksson T, et al. Estimated life years lost due to fatal late complications after photon or proton radiotherapy [Abstract]. ESTRO 11th Biennial On Physics & Radiation Technology For Clinical Radiotherapy ed. 2011 (in press).
[40] Bathia S, Ramsay NK, Bantle JP, Mertens A, Robison LL. Thyroid abnormalities after therapy for Hodgkin's disease in childhood. Oncologist 1996;1:62–7.
[41] Marks LB, Bentzen SM, Deasy JO, Kong FM, Bradley JD, Vogelius IS, et al. Radiation dose-volume effects in the lung. Int J Radiat Oncol Biol Phys 2010;76(3 Suppl):S70–6.
[42] Houweling AC, Philippens ME, Dijkema T, Roesink JM, Terhaard CH, Schilstra C, et al. A comparison of dose-response models for the parotid gland in a large group of head-and-neck cancer patients. Int J Radiat Oncol Biol Phys Epub 2009 Dec 10.
[43] Kal HB, Van Kempen-Harteveld ML. Induction of severe cataract and late renal dysfunction following total body irradiation: Dose-effect relationships. Anticancer Res 2009;29: 3305–9.
[44] Burman C, Kutcher GJ, Emami B, Goitein M. Fitting of normal tissue tolerance data to an analytic function. Int J Radiat Oncol Biol Phys 1991;21:123–35.
[45] Paddick I. A simple scoring ratio to index the conformity of radiosurgical treatment plans. Technical note. J Neurosurg 2000;93(Suppl 3):219–22.